

Real-time Agriculture Field Monitoring Using IoT-based Sensors and Unmanned Aerial Vehicles

Cong Hoang Quach
VNU University of
Engineering and Technology
Hanoi, Vietnam
hoangqc@vnu.edu.vn

Minh Trien Pham
VNU University of
Engineering and Technology
Hanoi, Vietnam
trienpm@vnu.edu.vn

Manh Duong Phung
University of Technology Sydney
Sydney, Australia
manhduong.phung@uts.edu.au

Abstract—This paper introduces a system to monitor agriculture fields in real time. It includes a sensor network for in situ data collection and an unmanned aerial vehicle (UAV) system for remote sensing. The sensor network uses a number of sensor nodes to measure different parameters of the plants and environment such as temperature, humidity, and nitrogen composition. For data communication, the sensor network uses LoRa, a low-power wide-area network modulation technique, that allows receiving signals from sensor nodes at a distance of up to 450 m for a single receiver. The UAV includes visual and near infrared cameras to collect photos of the field. The data collection is carried out automatically via a path planning process that takes into account the overlapping ratio and resolution of the photos. The data collected is then handled by a cloud server that allows users to access in real time via a web-based application and an application on smartphones. A number of experiments have been conducted with the system being tested in several agricultural sites to evaluate its practical applicability.

Index Terms—Crop monitoring, agriculture management, unmanned aerial vehicles, Internet of Things

I. INTRODUCTION

Continuous monitoring of field conditions and vegetation growth plays a key role in agriculture as it provides timely information to access essential physiological properties of plants such as vigor and biomass as well as detect problems related to their disease and nutrient deficiency. Current monitoring approaches can be categorized into site-based and remote sensing methods. The first approach uses in situ sensors connected via communication networks to monitor field conditions. In [1], a low power wireless sensor network (WSN) is used to collect temperature and humidity data of the crop environment and images of plant growth. Two types of nodes including point-based sensor nodes and image sensor nodes are used and the data transmission is carried out via a self-defined protocol named Collection Tree Protocol. Wireless sensor networks are also used in [2] to monitor different environmental conditions such as temperature, humidity, and water level to improve crop yield and quality. The system uses microcontrollers for data processing and Zigbee protocol for data communication. The Internet of Things (IoT) has been used in [3] to allow site-based sensor data to be monitored anywhere via a web browser. The system uses Arduino microcontrollers to collect data from sensors and Ethernet shields to transmit the data

over the Internet. WSN and IoT have also been used in [4]–[6] as the main data communication technologies in agriculture monitoring systems. This approach provides capabilities to continuously monitor a number of parameters of the field conditions. It however can only provide information at certain locations of the field. A prediction model is required to extend the results to other areas. Otherwise, dense sensor networks should be implemented which would significantly complicate the system design.

In the second approach, satellite and aerial images are used in combination with image processing techniques to analyze plant conditions. Sakamoto et al. [7] use visible and near infrared images captured from two compact digital cameras to evaluate vegetation indices including the normalized difference vegetation index (NDVI), the simple ratio index (SR), and the green chlorophyll index (CI_{green}). Equations for calculating the indices are obtained based on finding the nonlinear relationship between the pixel values and the intensity of incident light. In [8], a data fusion model using images collected from unmanned aerial vehicles (UAVs) and satellites is proposed for crop monitoring. The model extracts canopy spectral information from satellite data and canopy structure information from UAV data and then uses machine learning to evaluate properties of soybean plants such as leaf area index (LAI) and aboveground biomass (AGB). In [9], a system that is capable of reconstructing a 4D model of a crop is introduced. That model contains not only the spatial information of plants such as canopy size, height, and leaf color but also their temporal information such as the growth rate and leaf color transition. The system uses data collected from various sensors as the input to a data association algorithm to generate the 4D model. Remote sensing is also used in [10]–[13] as an effective non-invasive method to monitor and evaluate different properties of plants. This method however typically provides periodic rather than continuous monitoring due to intermittent data collection provided by satellites and UAVs. In addition, it faces difficulties in evaluating environmental parameters such as soil humidity or water level. It is therefore necessary to combine both the site-based and remote sensing methods to provide a complete system for agricultural field monitoring.

In this study, we propose a system that is capable of monitoring not only the spatio-temporal information of the

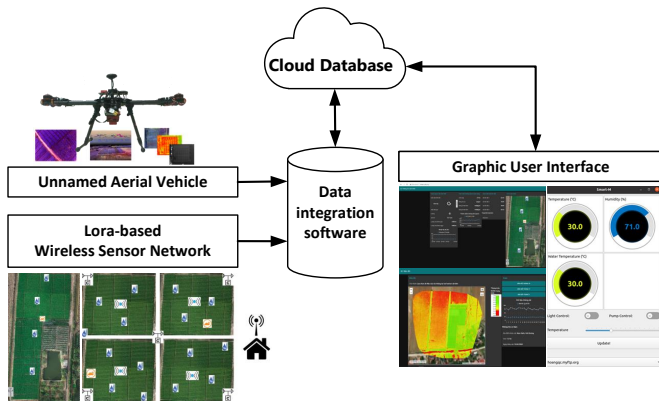


Fig. 1: Overview of the proposed system

agricultural field but also environmental parameters in real time. The system exploits IoT technology to form a network of sensors for environmental data collection. It also includes UAVs equipped with visible and near infrared (NIR) cameras to acquire images of the plants. For data processing, we have developed a path planning algorithm that calculates viewpoints for the UAV to follow and take pictures and a system to process the collected data to extract necessary information about the environment and plant conditions. We also develop an application for smartphones and a web-based interface to make the data accessible in real time for timely decision making. A number of experiments and evaluations have been conducted and results confirm the effectiveness and validity of our approach.

II. PROPOSED SYSTEM

Figure 1 shows an overview of our proposed system which includes an IoT-based sensor network, UAVs, a cloud computing system, a data processing system, and a user interface. Details of the main components are described as follows.

A. IoT-based sensor network

The sensor network includes a number of modules installed in the field to measure environmental parameters. We choose the following sensor modules for the typical needs of agricultural monitoring:

- **Meteorological sensor module for weather monitoring:** This module includes the sensors to monitor the weather of the farming area such as temperature, humidity, wind direction, wind speed, and rainfall. These are the factors that greatly affect the plant growth in both short-term and long-term.
- **Light sensor module:** This module measures light intensity in three bands including visible, near-infrared and ultraviolet. It allows the system to monitor the lighting condition to evaluate if the plant photosynthesis is suitable for their growth.
- **Air quality module:** This module measures changes in nitrogen composition such as NH_3 and NO_2 which is important to determine the time for using nitrogen



Fig. 2: Cameras and drones used. (a) Camera Sentera Quad Sensor installed on the drone DJI M600 Pro; (b) Camera MapIR Survey 3 installed on Phantom 4 Pro

fertilization in the farming area. The module also monitors the level of O_2 and CO_2 which is important for the growth of some plant species such as button mushroom and reishi mushroom.

Data from the sensors is transmitted to the base station before being forwarded to the Internet. We use the network modulation technique LoRa for energy efficiency and long range communication. The messaging protocol used is MQTT, a standard protocol for IoT to connect remote sensors with minimal network bandwidth. The communication system is developed with an open design so that parameters such as the data frame, transmission time, and quality of service (QoS) can be modified. The sensor network is thus scalable to the number of sensor nodes and network coverage.

B. UAV system for data collection

To collect remote sensing data of the field, we use cameras installed on UAVs with the following configurations:

- (1) Camera Micasense installed on the UAV using a passive anti-vibration mechanism which is a soft rubber of 3 mm thick.
- (2) Camera Sentera Quad Sensor installed on the drone DJI M600 Pro with an active 3D gimbal stabilizer.
- (3) Camera MapIR Survey 3 installed on the drone Phantom 4 using a 3D printed plastic and soft rubber for anti-vibration.

In our system, configuration 1 is designed for high quality photos in which the high sensitivity camera is directly integrated into the flight controller. Configuration 2 is suitable for operating in unstable weather conditions since it has the high safety factor and good anti-vibration capability as shown in Fig.2a. Configuration 3 is a combination of low-cost cameras and drones as shown in Fig.2b. This configuration, if being properly implemented, can provide images at almost the same quality as the two configurations above at a lower cost.

C. Data processing

Data processing module is the main component of our system. It carries out the radiometric calibration for cameras, plans flight paths for UAV and handle the data collected from sensors.

1) *Radiometric Calibration*: To calculate the normalized difference vegetation index (NDVI) and the normalized difference red edge (NDRE) for plant monitoring, it is necessary to determine the reflection ratio of the NIR and RED bands. However, lighting conditions often change during the surveying process leading to differences in the power spectral density at these two bands and hence the reflected intensity. Therefore, it is necessary to calculate the power ratio of NIR and RED before flying.

In this study, we propose to use the calibration target method in which we place a reflector with 50-51% reflectivity, as shown in Fig.3, next to the UAV takeoff and landing point to take pictures between the two surveys. Based on the marker, the calibration algorithm can detect the reflector and hence all the pixels I within that reflector. According to [14], the value of pixel I for a certain band is given by:

$$I = P \cdot R \cdot C, \quad (1)$$

where I is the pixel value ranging from 0 to 255, P is the power spectrum, R is the reflectance coefficient associated to the reflector used as shown in Table I, and C is the optic property of the camera.

Since the camera configuration is fixed, the reflection ratio is given by:

$$\frac{I_{nir}}{I_{red}} = \frac{P_{nir} \cdot R_{nir} \cdot C}{P_{red} \cdot R_{red} \cdot C} = \frac{P_{nir} \cdot R_{nir}}{P_{red} \cdot R_{red}} \quad (2)$$

The overall ratio then can be computed by including all the detected pixels of the calibration target:

$$\delta = \frac{P_{nir}}{P_{red}} = \frac{\sum I_{nir} \cdot R_{nir}}{\sum I_{red} \cdot R_{red}} \quad (3)$$

Finally, the NDVI can be estimated as:

$$NDVI = \frac{I_{nir} - \delta \cdot I_{red}}{I_{nir} + \delta \cdot I_{red}} \quad (4)$$

Similarly, the NDRE can be computed as:

$$NDRE = \frac{I_{nir} - \delta_{NDRE} \cdot I_{re}}{I_{nir} + \delta_{NDRE} \cdot I_{re}}, \quad (5)$$

where

$$\delta_{NDRE} = \frac{P_{nir}}{P_{re}} = \frac{\sum I_{nir} \cdot R_{nir}}{\sum I_{re} \cdot R_{re}} \quad (6)$$

TABLE I: Reflectance coefficients of the calibration target RP04 Micasense

| | RED | RE (Red edge) | NIR |
|-------------------------|--------|---------------|--------|
| Wavelength | 668 nm | 717 nm | 840 nm |
| Bandwidth | 20 nm | 10 nm | 40 nm |
| Reflectance coefficient | 52.0 % | 52.0 % | 51.8 % |



Fig. 3: The Micasense's reflector used for radiometric calibration

2) *Path planning*: To capture photos of the field, it is important to plan a path for the UAV to follow that includes the viewpoints at which the camera takes photos. The viewpoints should be selected so that the photos taken cover the whole area of interest. The calculation of viewpoints in this work is similar to our previous work [15]. Specifically, the survey area is split into a set of geometric primitives p as shown in Fig.4. The size of p is equivalent to the effective field of view of the camera. Let s_f be the required resolution or the smallest feature being distinguished in the captured photo and r_c be the resolution of the camera. As illustrated in Fig.5, the field of view of the camera, a_{fov} , is computed as:

$$a_{fov} = \frac{1}{2} r_c s_f. \quad (7)$$

Since the captured photos need to overlap by a percentage o_p for the sticking algorithm to merge them, the effective field of view of the camera p is computed as:

$$p = (1 - o_p) a_{fov}. \quad (8)$$

To obtain p from each captured photo, the working distance from the camera to the surveying surface is computed as:

$$d_k = \frac{a_{fov} f}{s_s}, \quad (9)$$

where f is the focal length and s_s is the sensor size of the camera. The viewpoints then can be selected as the centers of geometric primitives p projected to the surface having the distance d_k to the surveying surface as illustrated in Fig.4. Those viewpoints can be chosen as waypoints for the flight path of the UAV.

D. Cloud server and user applications

To handle the collected data and provide users with real-time access, we use a cloud server as the center for monitoring and control. This server manages data from measuring stations and sensor nodes as well as classifying and storing the collected data. It also handles the access requests relating to the environmental data and broadcasts messages relating to actions required for the farm.

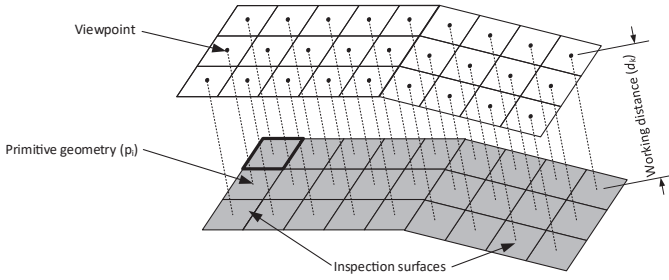


Fig. 4: Viewpoint selection

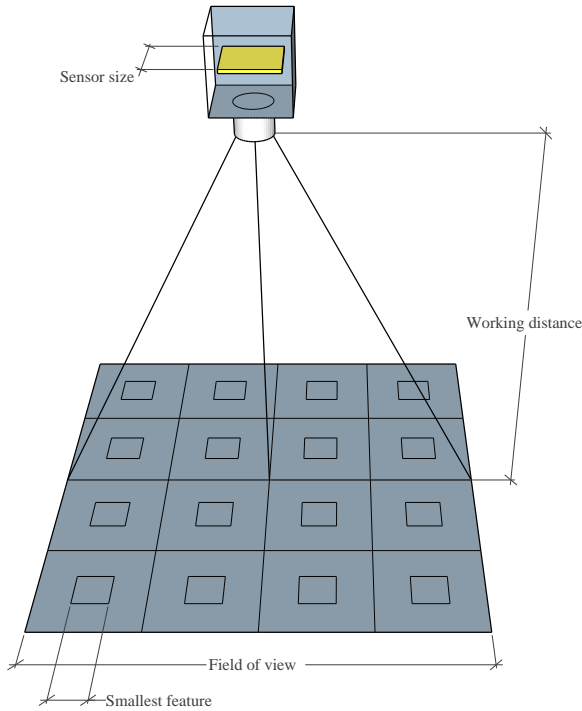


Fig. 5: Camera setup for data collection

Our system provides two means of access for users including a web-based graphic user interface and an application on smartphones. We use Node-Red, a flow-based development tool, to develop the web-based application. It reads MQTT packets, stores them in the MongoDB database, and generates daily and weekly reports as shown in Fig.6. The mobile application is developed using the Qt platform and provides similar functions as with the web-based application.

III. EXPERIMENTS

We have tested our system in several agricultural sites to evaluate its performance with details as follows.

A. Experimental setup

In our system, we use the weather station of DFRobot that includes sensors for temperature, humidity, wind speed, wind direction, and rainfall. The sunlight sensor used is Grove SKU 101020089 that can detect light in the ultraviolet (UV), visible, and NIR bands. To measure the air composition, we use the

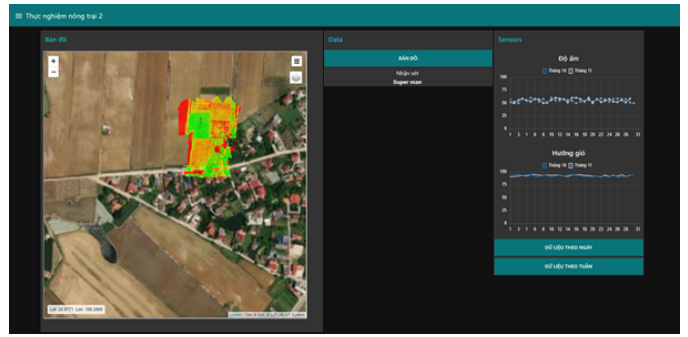


Fig. 6: The web-based graphic user interface



(a) Sensor box

(b) Weather station

Fig. 7: Sensor nodes installed at the field

MiCS-6814 module of Amphenol SGX Sensortech. For the LoRa network, we use Dragino LoRa shields for sensor nodes and Dragino Gateway LG01 modules for stations. Figure 7 shows the sensor box and the weather station installed at the field. For remote sensing, the drones and cameras used are described in Section II-B.

Our system has been set up in several crops in northern Vietnam. The crop seasons and plants being monitored include:

- the spring-summer crop of maize in Hai Duong
- the winter-spring crop of tomato in Dong Anh
- the winter-spring crop of carrots in Hai Duong

We also tested our system at a mountainous area dedicated to organic farming in Ba Vi, Hanoi.

B. Results

1) *IoT-based sensor module*: We have installed the sensor network in the aforementioned crops and measured the communication ability of the sensor nodes. According to the manufacturer's specifications, the LoRa device we use has the spreading factor of 7, bandwidth of 125 kHz, and encoding rate of 4/5. In the experiment, we configured the device to operate at the frequency of 923 MHz and the transmitting power of 20 dBm. We used three antennas with the gains of 3 dBi, 10 dBi, and 18 dBi. The results were measured by the RF Explorer 915M V2.0 device. Figure 10 shows the receiving power with respect to the distance. It can be seen that the receiver we use, the LoRa Gateway OLG-01 with the sensitivity of -120 dBm, can communicate with the sensor nodes at the distance of 200

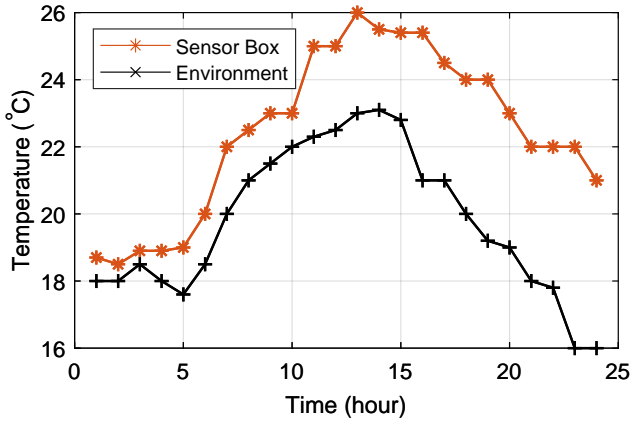


Fig. 8: Temperature of the environment and inside the device box

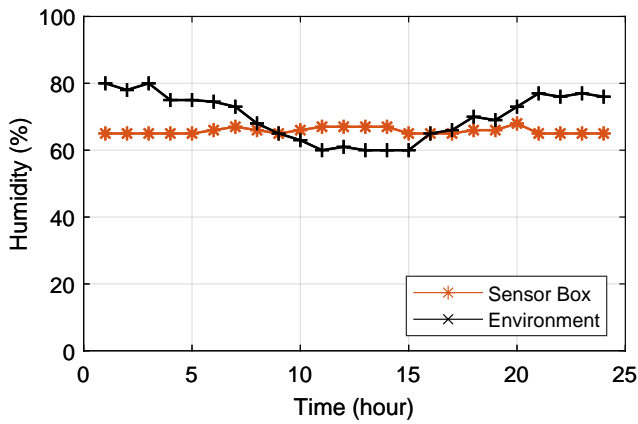


Fig. 9: Humidity of the environment and inside the device box

m for the 3 dBi antenna, 400 m for the 10 dBi antenna, and 450 m for the 18 dBi antenna. Therefore, a suitable antenna can be used depending on the size of the crop.

In another experiment, we measured the temperature and humidity of the environment and inside the device box as

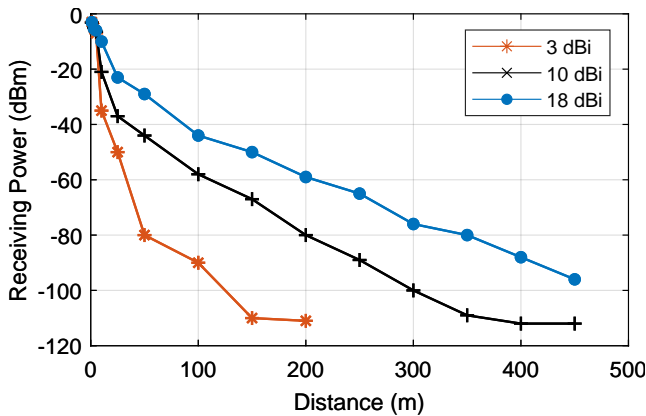


Fig. 10: The receiving power with respect to the distance of the LoRa network for three antennas

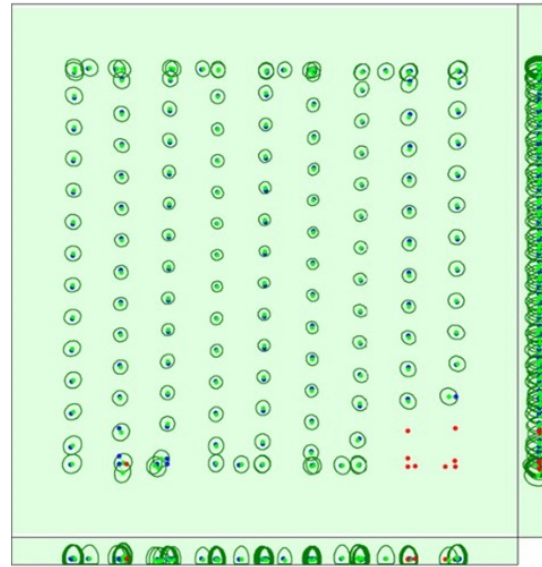


Fig. 11: The map showing the actual viewpoints and their variance (circle lines) in experiments

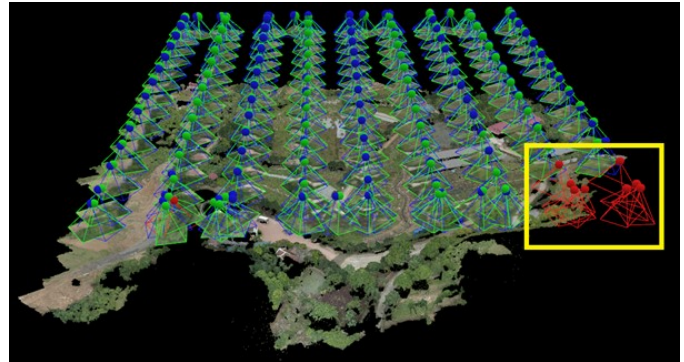


Fig. 12: The planned path for the UAV to collect data

shown in Fig.8 and Fig.9. The temperature inside the device box is higher than the outside environment which is reasonable due to the heat emitted from operating electronic components. It also explains the stable value of the humidity inside the box compared to the outdoor environment. More importantly, the relatively low temperature and humidity of the device imply its proper operation.

2) *UAV-based data collection results:* We have conducted experiments to evaluate the use of UAV for remote sensing data collection. Given the area to be surveyed and the parameters of the camera, the flight altitude and viewpoints can be computed as in Section II-C2. Those values are then used as input to the Pix4Dcapture software to create a flight path for the UAV. In our experiments, we used the Phantom 4 Pro drone with an anti-vibration system for the camera to survey an area of 5.8 ha. Figure 12 shows the planned path and Fig.11 shows the actual viewpoints (the points at which the camera takes photos) together with their variance during the flight. It can be seen that planned and actual viewpoints match relatively well

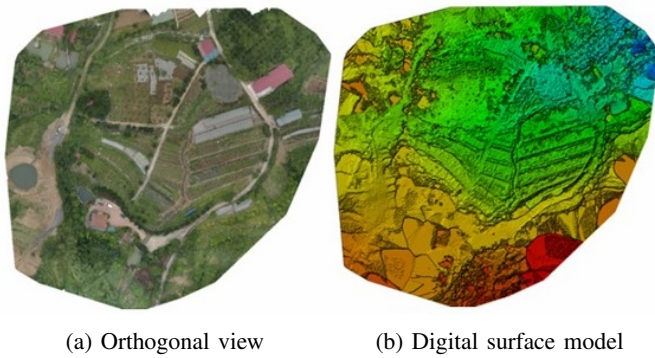


Fig. 13: The reconstructed models of the surveying area

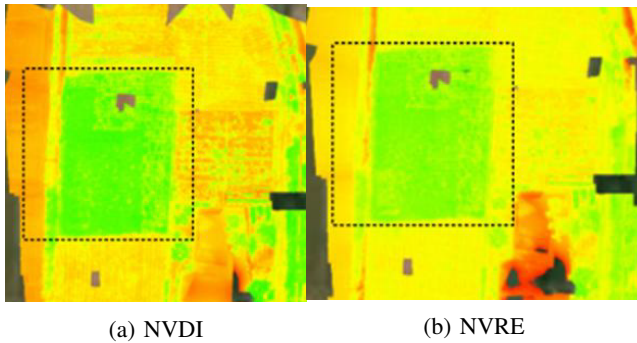


Fig. 14: The estimated vegetation indices

despite small errors caused by GPS and changes in the surface height. It is also noticeable that some points (highlighted in red) do not meet the requirement on the overlapping ratio due to their large errors. Despite that, the photos taken were successfully stuck together to provide an overall orthogonal view of the surveying area as shown in Fig.13a and the digital surface model of the area as shown in Fig.13b.

Figure 14 shows the estimated NVDI and NVRE for a farm. It can be seen that changes in the value of NVRE is greater than NVDI since NVRE is more sensitive to the chlorophyll, leaf area variation, and influence of substrate. As the result, NVRE is better to use during the mid- and late-season to get more information about the growth of plants.

IV. CONCLUSION

We have proposed in this work a system for real-time monitoring of agricultural sites using IoT-based sensors and UAVs. With the sensor network, we have designed the sensor modules together with a LoRa network using the Internet of Things technology for data communication. For UAVs, we have introduced the calculation of viewpoints for path planning and a method to calibrate the reflection levels for NDVI and NDRE indices. In addition, a web-based application and an application for smartphones have been developed for real-time access of monitoring data. Our system has been tested in several agricultural sites and the results confirm its effectiveness and validity for monitoring and management tasks.

ACKNOWLEDGMENT

The author Cong Hoang Quach is supported by the Domestic Ph.D. Scholarship Programme of Vingroup Innovation Foundation (VINIF), Vingroup Big Data Institute (VINBIG-DATA), code VinIF 2020. TS.23.

REFERENCES

- [1] Z. Liqiang, Y. Shouyi, L. Leibo, Z. Zhen, and W. Shaojun., "A crop monitoring system based on wireless sensor network," *Procedia Environmental Sciences*, vol. 11, pp. 558–565, 2011.
- [2] B. B. Bhanu, K. R. Rao, J. Ramesh, and M. A. Hussain, "Agriculture field monitoring and analysis using wireless sensor networks for improving crop production," in *2014 Eleventh International Conference on Wireless and Optical Communications Networks (WOCN)*, 2014, pp. 1–7.
- [3] I. Mohanraj, K. Ashokumar, and J. Naren, "Field monitoring and automation using iot in agriculture domain," *Procedia Computer Science*, vol. 93, pp. 931–939, 2016.
- [4] L. Dan, C. Xin, H. Chongwei, and J. Liangliang, "Intelligent agriculture greenhouse environment monitoring system based on iot technology," in *2015 International Conference on Intelligent Transportation, Big Data and Smart City*, 2015, pp. 487–490.
- [5] F. Viani, M. Bertolli, M. Salucci, and A. Polo, "Low-cost wireless monitoring and decision support for water saving in agriculture," *IEEE Sensors Journal*, vol. 17, no. 13, pp. 4299–4309, 2017.
- [6] O. Chieochan, A. Saokaew, and E. Boonchieng, "Iot for smart farm: A case study of the lingzhi mushroom farm at maejo university," in *2017 14th International Joint Conference on Computer Science and Software Engineering (JCSSE)*, 2017, pp. 1–6.
- [7] T. Sakamoto, A. A. Gitelson, A. L. Nguy-Robertson, T. J. Arkebauer, B. D. Wardlow, A. E. Suyker, S. B. Verma, and M. Shibayama, "An alternative method using digital cameras for continuous monitoring of crop status," *Agricultural and Forest Meteorology*, vol. 154–155, pp. 113–126, 2012.
- [8] M. Maimaitijiang, V. Sagan, P. Sidike, A. M. Daloye, H. Erkbol, and F. B. Fritsch, "Crop monitoring using satellite/UAV data fusion and machine learning," *Remote Sensing*, vol. 12, no. 9, 2020.
- [9] J. Dong, J. G. Burnham, B. Boots, G. Rains, and F. Dellaert, "4d crop monitoring: Spatio-temporal reconstruction for agriculture," in *2017 IEEE International Conference on Robotics and Automation (ICRA)*, 2017, pp. 3878–3885.
- [10] P. Defourny, S. Bontemps, N. Bellemans, C. Cara, G. Dedieu, E. Guzonato, O. Hagolle, J. Inglada, L. Nicola, T. Rabaute, M. Savinaud, C. Udroui, S. Valero, A. Begues, J.-F. Dejoux, A. El Harti, J. Ez-zahar, N. Kussul, K. Labbassi, V. Lebourgeois, Z. Miao, T. Newby, A. Nyamugama, N. Salh, A. Shelestov, V. Simonneaux, P. S. Traore, S. S. Traore, and B. Koetz, "Near real-time agriculture monitoring at national scale at parcel resolution: Performance assessment of the sen2-agri automated system in various cropping systems around the world," *Remote Sensing of Environment*, vol. 221, pp. 551–568, 2019.
- [11] N. Sanchez, A. Gonzalez-Zamora, J. Martinez-Fernandez, M. Piles, and M. Pablos, "Integrated remote sensing approach to global agricultural drought monitoring," *Agricultural and Forest Meteorology*, vol. 259, pp. 141–153, 2018.
- [12] X. Zhang, F. Zhang, Y. Qi, L. Deng, X. Wang, and S. Yang, "New research methods for vegetation information extraction based on visible light remote sensing images from an unmanned aerial vehicle (uav)," *International Journal of Applied Earth Observation and Geoinformation*, vol. 78, pp. 215–226, 2019.
- [13] A. Kern, Z. Barcza, H. Marjanovic, T. Arendas, N. Fodor, P. Bonis, P. Bogner, and J. Lichtenberger, "Statistical modelling of crop yield in central europe using climate data and remote sensing vegetation indices," *Agricultural and Forest Meteorology*, vol. 260–261, pp. 300–320, 2018.
- [14] D. Olsen, C. Dou, X. Zhang, L. Hu, H. Kim, and E. Hildum, "Radiometric calibration for AgCam," *Remote Sensing*, vol. 2, no. 2, pp. 464–477, 2010.
- [15] M. D. Phung, C. H. Quach, T. H. Dinh, and Q. Ha, "Enhanced discrete particle swarm optimization path planning for UAV vision-based surface inspection," *Automation in Construction*, vol. 81, pp. 25–33, 2017.